Interdiscip Sci Comput Life Sci (2013) 5: 1–12
DOI: 10.1007/s12539-013-0147-z

Docking and *in silico* ADMET Studies of Noraristeromycin, Curcumin and Its Derivatives with *Plasmodium falciparum* SAH Hydrolase: A Molecular Drug Target against Malaria

Dev Bukhsh SINGH[1*], Manish Kumar GUPTA[2], Durg Vijay SINGH[2], Sushil Kumar SINGH[3], Krishna MISRA[4]
[1](Department of Biotechnology, Institute of Biosciences and Biotechnology, Chhatrapati Shahu Ji Maharaj University, Kanpur 208024, Uttar Pradesh, India)
[2](Department of Bioinformatics, University Institute of Engineering and Technology, Chhatrapati Shahu Ji Maharaj University, Kanpur 208024, Uttar Pradesh, India)
[3](Centre for Cellular and Molecular Biology, Hyderabad 500007, Andhra Pradesh, India)
[4](Indian Institute of Information Technology, Allahabad 211012, Uttar Pradesh, India)

Received 8 March 2012 / Revised 4 May 2012 / Accepted 6 August 2012

Abstract: The *Plasmodium falciparum* S-adenosyl-L-homocysteine hydrolase (pfSAHH) enzyme has been considered as a potential chemotherapeutic target against malaria due to the amino acid differences found on binding sites of pfSAHH related to human SAHH. It has been reported that noraristeromycin and some curcumin derivatives have potential binding with the largest cavity of pfSAHH, which is also related to the binding with Nicotinamide-Adenine-Dinucleotide (NAD) and Adenosine (ADN). Our present work focuses on docking and ADMET studies to select potential inhibitors of pfSAHH. The binding of the selected inhibitor of the PfSAHH active site was analyzed using Molegro Virtual Docker. In this study, curcumin and its derivatives have been found to have higher binding affinity with pfSAHH than noraristeromycin. Seven amino acid residues Leu53, His54, Thr56, Lys230, Gly397, His398 and Phe407 of pfSAHH involved in binding with curcumin, are the same as those for noraristeromycin, which reveals that curcumin and noraristeromycin bind in the same region of pfSAHH. Curcumin has shown a strong interaction with hydrophobic amino acid residues of pfSAHH. Molecular Docking and ADMET predictions suggest that curcumin can be a potent inhibitor of pfSAHH with ability to modulate the target in comparatively smaller dose. Therefore, curcumin is likely to become a good lead molecule for the development of effective drug against malaria.
Key words: pfSAHH, malaria, noraristeromycin, curcumin, docking, ADMET, anti-malarial.

1 Introduction

S-adenosyl-L-homocysteine hydrolase (SAHH) is a cellular enzyme that catalyses the hydrolysis of SAH (S-Adenosyl-L-Homocysteine) to ADN and homocysteine *in vivo*. It plays a very important role in regulation of biological methylation process (Yuan *et al.*, 1999). The SAH is a potent feedback inhibitor of SAM-dependent biological methylation such as the 5'-end of eukaryotic mRNA. The eukaryotic mRNA must possess a methylated 5'-cap structure for stability against phosphatases and ribonucleases, for proper binding to ribosome, and for the promotion of splicing. Therefore, normal protein expression is prevented by synthesizing an uncapped mRNA (Kitade *et al.*, 2000). As a result SAH hydrolase can be selected as a therapeutic target to cure so many diseases such as malaria, cancer, inflammation, viral and cardiovascular diseases. Carbocyclic and acyclic nucleosides possessing 2-fluoroadenine derivatives also have inhibitory activities against pfSAHH (Kitade *et al.*, 2003b). Inhibitors of SAH hydrolase affect the methylation process of nucleic acids, proteins and small molecules. Conventional drugs are not very much effective against malaria due to emergence of new strains of *Plasmodium falciparum*. Inhibitors of pfSAHH may prove to be new therapeutic drug against malaria.

Noraristeromycin analogues such as $3',4'$-anhydronoraristeromycins and 2-amino-$3',4'$-anhydronoraristeromycin have been synthesized and their inhibitory activity against human and *Plasmodium falciparum* SAH hydrolase has been

*Corresponding author.
E-mail: answer.dev@gmail.com

reported. Amongst these, $3', 4'$- anhydronoraristeromycin has shown very high inhibitory activity against human SAHH (hsSAHH) (Kojima *et al.*, 2002). The inhibitory activities of $4'$-modified noraristeromycins analogs, $4'$-sulfo-, $4'$-sulfamoy, $4'$-azido and $4'$-amino-noraristeromycin and related compounds against pfSAHH are well known (Ando *et al.*, 2008). 2-Fluoronoraristeromycin shows significant inhibitory activity against recombinant pfSAHH. The inhibitory activities of noraristeromycin derivatives possessing 2- or 8-position modified adenine or 8-aza-7-deazaadenine against pfSAHH were studied. Among these 2-aminonoraristeromycin has selectively shown inhibitory activity against pfSAHH (Kitade *et al.*, 2003a). Curcumin is a yellow colored pigment obtained from the rhizome of turmeric. It has a wide range of therapeutic activities. Being herbal in nature it has fewer side effects. Curcumin is a potential candidate for the development of adjunctive therapy for cerebral malaria (Mimche *et al.*, 2011). It has been reported that curcumin in combination with artemisinin and piperine has synergistic and positive interaction effect on anti-plasmodial activity (Tagboto *et al.*, 2001; Rasoanaivo *et al.*, 2011). *In vitro* and *in vivo* study reveals that artemisinin-type compounds are found active towards protozoal, viral diseases and cancer cells (Efferth *et al.*, 2011).

Artemisinin and its analogues bind to a hydrophobic pocket located in the transmembrane region of PfATP6 (modeled) and interfere with calcium transport (Naik *et al.*, 2011). The pfATP6 is considered the putative target for the anti-malarial drug artemisinin and its derivatives (Jung *et al.*, 2005). The modeled structure of pfATP6 was docked with artemisinin and its derivatives, but no correlation has been found between *in silico* binding affinity and *in vitro* anti-malarial activity (Garah *et al.*, 2009). Docking studies of curcumin, artemisinin and its analogues have been done with modeled structure of pfATP6, since there is no X-ray crystallographic or NMR structure of pfATP6 available in the PDB database.

NAS-21(4,4,4-trifluoro-1-(4-nitrophenyl) butane-1,3-dione) and NAS-91 (4-chloro-2-[(5-chloroquinolin-8-yl)oxy]phenol) cause significant inhibition of pfFabZ (plasmodium falciparum β-hydroxyacyl-acyl carrier protein dehydratase) (Sharma *et al.*, 2003). Gossypol derivatives and naphthoic acid-based compounds have shown inhibition of *Plasmodium falciparum* lactate dehydrogenase (pfLDH), but clinically relevant candidate molecule is not yet available (Brady *et al.*, 2004).

Purine nucleoside phosphorylase from *Plasmodium falciparum* (PfPNP) is an anti-malarial target, which converts inosine or 5'-methylinosine to hypoxanthine. Immucillin-H is a potent inhibitor of PNP, and kills the *Plasmodium falciparum* in culture. 5'-Methylthioimucillin-H has been developed as a potent and selective inhibitor PfPNP (Shi *et al.*, 2004). Threonine peptidases have been also reported as a drug target against malaria (Tschan *et al.*, 2011).

In the present work, comparative docking study of noraristeromycin and curcumin derivatives has been performed with hsSAHH and pfSAHH, and binding mode of inhibitors with the pfSAHH was investigated. Principal descriptors/ADME (Absorption, Distribution, Metabolism and Excretion) and toxicity values for inhibitors have been predicted.

2 Materials and methods

2.1 Target preparation

The three-dimensional structure of pfSAHH (1V8B) and hsSAHH (1LI4) was retrieved from the Protein Data Bank (www.rcsb.org). PDB file of PfSAHH (1V8B) contains a complex of pfSAHH with NAD and ADN, and has four chains A, B, C and D. The chain A (479 amino acid residues) of pfSAHH was separated from its ADN and NAD complex and was used for docking study. PDB file of hsSAHH (1LI4) is a complex of hsSAHH with NAD and Neplanocin (NOC).

2.2 Retrieval and preparation of ligand molecules

Physico-chemical properties and 2D structure (Fig. 1) of noraristeromycin and curcumin derivatives were retrieved from PubChem database of NCBI (National Center for Biotechnology Information) (http://pubchem.ncbi.nlm.nih.gov). Chemical formula, SMILES (Simplified Molecular Input Line Entry System) notation, molecular weight, LogP (partition coefficient), hydrogen bond donor, and hydrogen bond acceptor information for noraristeromycin and curcumin derivatives have been taken from PubChem. Compound ID (CID) can be used to retrieve more detailed information about compounds. 3D structures of curcumin and its derivatives were designed through CORINA server. CORINA is an online server that automatically generates three dimensional atomic coordinates from the constitution of a molecule (Sadowski *et al.*, 1994). Input to the CORINA server is SMILES notation of molecule (http://www.molecularnetworks.coml).

2.3 Docking approach

Molegro Virtual Docker (MVD) 2007.2.0.0 was used for docking study. MVD requires a 3D structure of both protein and ligand. MVD performs flexible ligand docking, so the optimal geometry of the ligand is determined during the docking (Thomsen *et al.*, 2006). The candidates with the best conformational and energetic results were selected. MVD (Thomsen *et al.*, 2006) was used to calculate the interaction energies between ligands and macromolecular systems from the 3D structures of the protein and ligands. The algorithm used was the MolDock Score, an adaptation of the Differen-

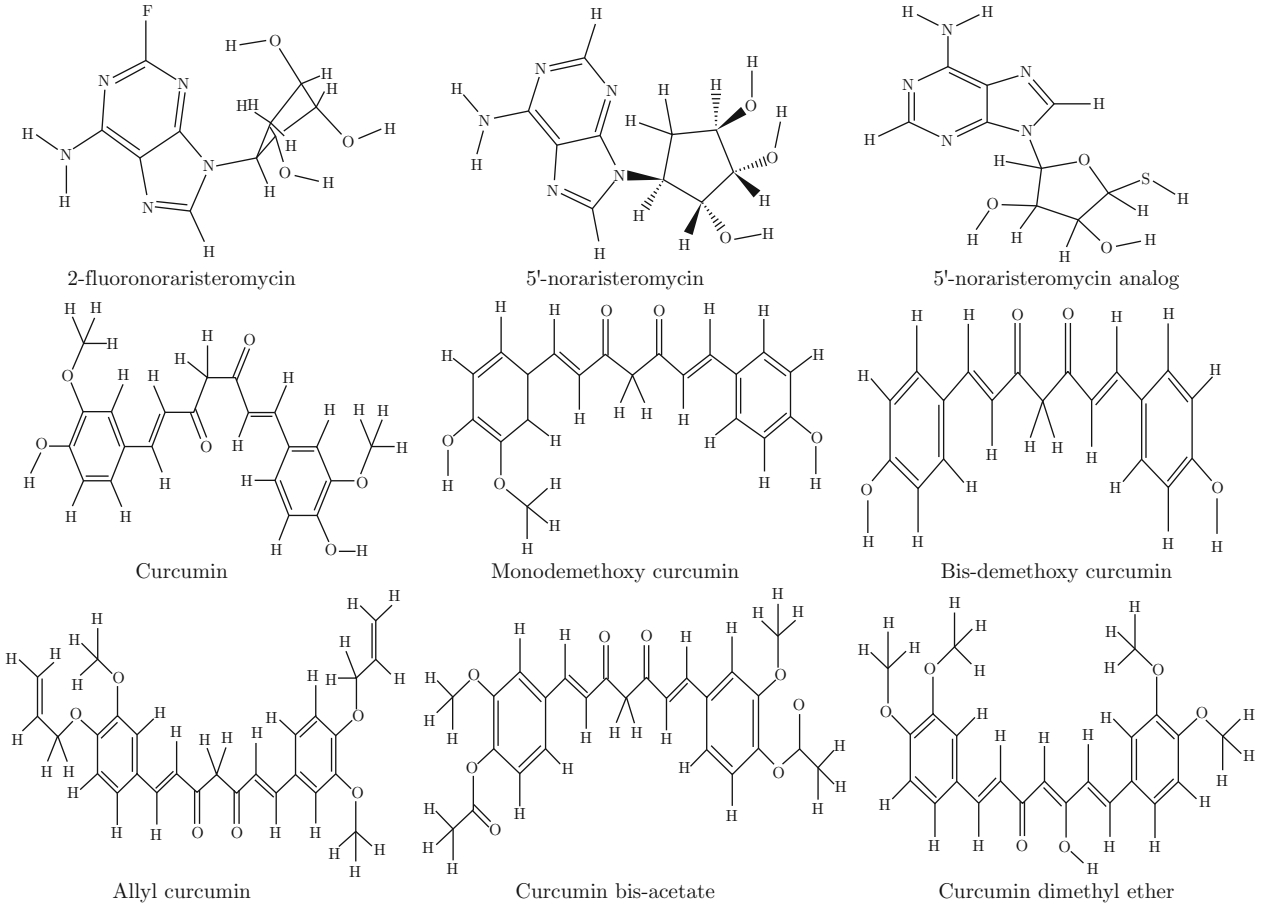

Fig. 1 Structure of norariste romycin and curcumin derivatives.

tial Evolution (DE) algorithm (Thomsen *et al.*, 2006); the MolDock Score energy, E_{score}, is defined by Equation 1, where E_{inter} is the ligand-protein interaction energy and E_{intra} is the internal energy of the ligand. E_{inter} is calculated according to Equation 2.

$$E_{score} = E_{inter} + E_{intra} \quad (1)$$

$$E_{inter} = \sum_{i\ ligand} \sum_{j\ protein} \left[E_{PLP}(\gamma_{ij}) + 332.0 \frac{q_i q_j}{4r_{ij}^2} \right] \quad (2)$$

The E_{PLP} term is a "piecewise linear potential" (Yang *et al.*, 2004) using two different parameters, one for the approximation of the steric term such as van der Waals between atoms and another for the potential for hydrogen bonds; it describes the electrostatic interactions between charged atoms (Thomsen *et al.*, 2006). E_{intra} is defined by Equation 3.

$$E_{intra} = \sum_{i\ ligand} \sum_{j\ protein} [E_{PLP}(\gamma_{ij})] + \sum_{flexible\ bonds} A[1 - cos(m\theta - \theta)] + E_{clash} \quad (3)$$

The first term in Equation 3 calculates the total energies involving pairs of atoms of the ligand, except those connected by two bonds. The second term stands for the torsional energy, where θ is the torsional angle of the bond. The average of the torsional energy bond contributions is used if several torsions have to be determined. The term E_{clash} defines a penalty of 1 000 kcal/mol if the distance between two heavy atoms (more than two bonds apart) is smaller than 2.0 Å, ignoring infeasible ligand conformations (Thomsen *et al.*, 2006).

2.4 Principal descriptors and ADME properties

Schrodinger software (QikProp v3.3) was used for calculation of principal descriptors and prediction of ADME. The BOSS program and OPLS-AA force field were used to perform Monte Carlo statistical mechanics simulations on organic solutes in periodic boxes of explicit water molecule (Jorgensen, 1998). This process resulted in configurational averages for a number of descriptors, including hydrogen bond counts and solvent-accessible surface area (SASA). Correlation of these descriptors to experimentally determined properties was obtained, and then algorithms that mimic the full Monte Carlo simulations and produce comparable results were developed. SDF (Structural Data File) format of compounds was used as input to QikProp. Output of QikProp consists of a number of principal

descriptors and ADME predictions.

2.5 Toxicity prediction

The toxicity module of ADMET Predictor™ (http://www.simulations-plus.com/) enables models to be built using Artificial Neural Network (ANN). ADMET Predictor™ is a computer program designed to estimate ADMET (Absorption, Distribution, Metabolism, Elimination, and Toxicity) properties of drug-like chemicals from their molecular structures. The program requires 2D or 3D molecular structure information (SDF or MOL file), parses the structure and calculates the values of molecular descriptors. Next, the program uses the molecular descriptor values as inputs to independent mathematical models in order to generate estimates for each of the ADMET properties. The input data were "sdf" files of various chemical structures. Using these "sdf" files as input to the ADMET Predictor™, the following parameters were estimated: Maximum Recommended Therapeutic Dose (MRDD), cardiac toxicity-affinity towards hERG-encoded potassium channels, chronic carcinogenicity and mutagenicity, phospholipidosis and human liver adverse effects. The neural network ensemble models employed in ADMET Predictor™ treat marginally active (marginally toxic) compounds as active (toxic) by setting the Reporting Index (RI) cutoff value to 3.0. Therefore, molecules with RI < 3.0 are classified as inactive (nontoxic) and those with RI > 3.0 as active (http://www.simulations-plus.com).

3 Results and discussion

3.1 Prediction of binding site

Cavity detection algorithm is used dynamically for finding the cavities by search algorithm (guided differential evolution) to focus the search during the docking simulation. The volumes of cavities present in hsSAHH and pfSAHH were calculated by MVD tool (Thomsen *et al.*, 2006). The top three cavities present in pfSAHH and hsSAHH, and their volumes are shown in Table 1. The top three cavities and binding of NAD and ADN with cavity-1 are shown in Fig. 2(a). The largest cavity (cavity-1) having volume of 271.872 Å^3 is shown in Fig. 2(b). In majority of cases, cavity with the largest size and volumes is associated with binding site. Cavity-1 is associated with the binding of NAD and ADN, which provides strong background for cavity-1 to serve as binding site. The top three cavities with volume of 414.72, 83.456 and 26.624 Å^3 have been predicted in hsSAHH. Volume of cavity-1 in hsSAHH is 414.72 Å^3 (Fig. 3), which is much larger than cavity-1 of pfSAHH (271.872 Å^3). Cavity with the largest volume has been selected as binding site for both of the targets (pfSAHH and hsSAHH) during docking with MVD.

3.2 Molecular docking of noraristeromycin inhibitors with pfSAHH and hsSAHH

The crystal structure of hsSAHH contains intermediate analogue neplanocin A (NOC) with the analogue bound in its 3'-keto form at the active sites of all of its four subunits and the four tightly bound cofactors (NAD) in their reduced (NADH) state (Yang *et al.*, 2003). Neplanocin A, a strong inhibitor of SAHH is reported to be a growth inhibitor of *Plasmodium falciparum* (Tanaka *et al.*, 2004).

The pfSAHH enzyme, in its active form, is homotetramer of identical subunits, each of which comprises of 479 amino acid residues and contains a tightly but

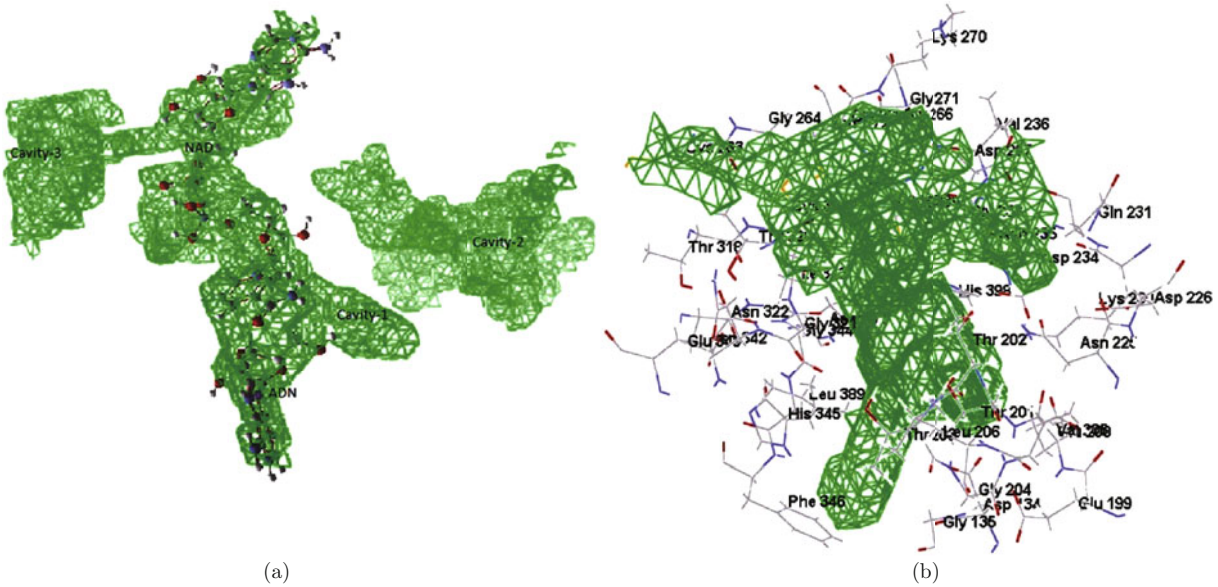

(a) (b)

Fig. 2 (a) Binding site for NAD and ADN in cavity-1. (b)Cavity-1 and surrounding residues predicted by MVD tool in pfSAHH.

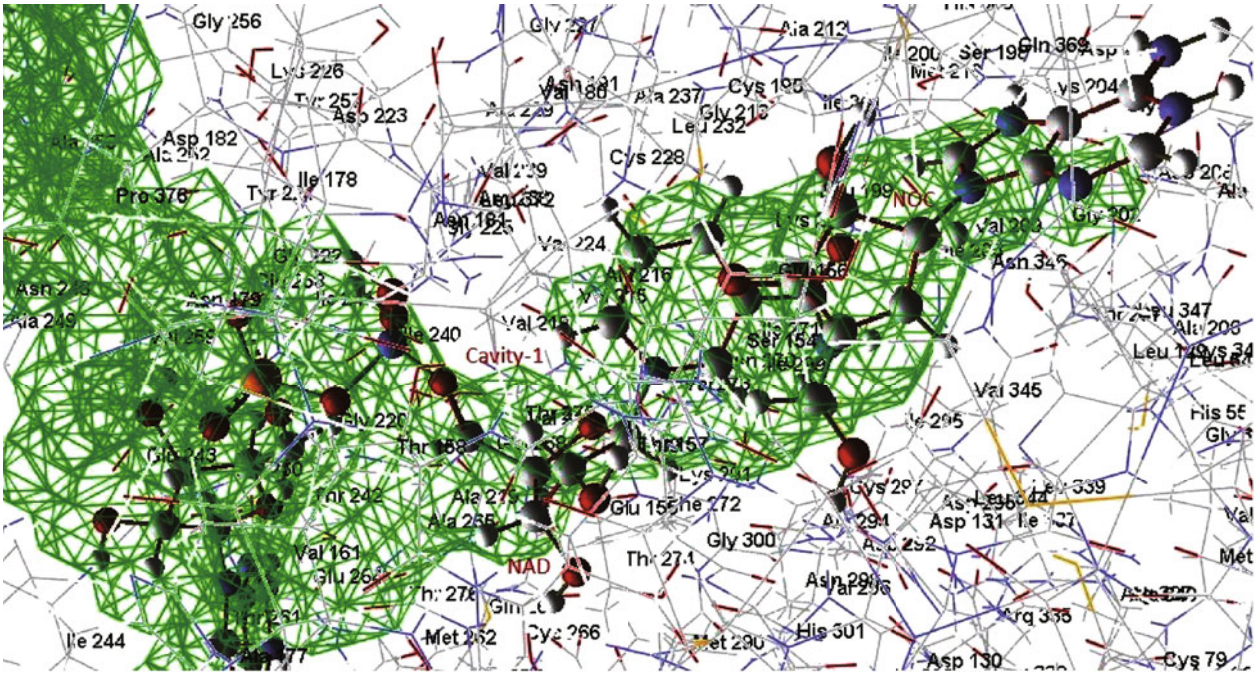

Fig. 3 Binding site for NAD and NOC in the largest cavity-1 and surrounding residues predicted by MVD tool in hsSAHH.

Table 1 Volumes of top 3 cavities predicted by MVD in Chain-A of pfSAHH and hsSAHH

S. No.	Top 3 cavities	Volume of cavities in pfSAHH (Å^3)	Volume of cavities in hsSAHH (Å^3)
1	Cavity-1	271.872	414.720
2	Cavity-2	220.160	83.456
3	Cavity-3	131.584	26.624

not covalently bound NAD cofactor (Tanaka *et al.*, 2004). The structural comparison of pfSAHH with hsSAHH reveals that a single substitution between the pfSAHH (Cys59) and hsSAHH (Thr60) accounts for the differential interactions with nucleoside inhibitors (Tanaka *et al.*, 2004). These structural differences between pfSAHH and hsSAHH may provide the valuable clues for development of anti-malarial drugs.

Noraristeromycin inhibitors were docked with hsSAHH and pfSAHH, and their binding energies with pfSAHH were calculated. Docking energies of noraristeromycin inhibitors with hsSAHH pfSAHH are given in Table 2 and Table 3. All noraristeromycin inhibitors have shown lower affinity for binding with hsSAHH than pfSAHH. The 2-fluoronoraristeromycin is showing high binding affinity for pfSAHH, and forms the very low energy complex (−125.58 kcal/mol) as compared to other noraristeromycin inhibitors. It forms twelve hydrogen bonds (−16.28 kcal/mol) with different amino acid residues of pfSAHH. 5′-Noraristeromycin and 5′-noraristeromycin analogues also form low energy complexes (−108.50 kcal/mol and −122.55 kcal/mol respectively) with pfSAHH, and significant contribution of hydrogen bond energy (−10.64 kcal/mol) and (−11.81 kcal/mol) respectively. Comparative docking study of noraristeromycin inhibitors with hsSAHH and pfSAHH reveals that pfSAHH can be energetically favorable and biologically significant drug target against malaria.

3.3 Molecular docking of curcumin and its derivatives with pfSAHH and hsSAHH

Curcumin, noraristeromycin and their derivatives were docked with PfSAHH to evaluate their binding efficiency. The motivation behind this was to investigate that anti-malarial effect of curcumin may be due to its binding with pfSAHH rather than PfATP6. The pfSAHH is an effective target for anti-malarial drugs. It has been reported that curcumin inhibits chloroquine-resistant *Plasmodium falciparum* growth in culture with an IC_{50} of approximately 5 μM (Reddy *et al.*, 2005). Anti-malarial effect of curcumin was predicted due to inhibition of *Plasmodium falciparum* ATP6 (pfATP6) (Ji *et al.*, 2009). PfATP6 is a sarcoplasmic reticulum, calcium-dependent ATPase of *Plasmodium falciparum*. Padmanaban *et al.* (2007) have reported that curcumin interacts with PfATP6 mainly through hydrophobic interactions and hydrogen bonds, which reveals that anti-malarial effect of curcumin may be due to its binding with pfATP6. Both docking studies of curcumin have been performed on modeled structure of pfATP6 since there is no x-ray or NMR structure of pfATP6 available. Anti-malarial effect of curcumin was reported in many literature reports, and a few targets have been hypothesized. But its exact target is

Table 2 Docking energies of noraristeromycin inhibitors with hsSAHH

S. No.	Noraristeromycin inhibitors (Top scoring only)	CID	Binding with hsSAHH (kcal/mol)			
			Total Energy	H-Bond	v.d.w.	Steric
1	2-Fluoronoraristeromycin	9993207	−109.58	−11.54	−33.26	−102.42
2	5′-Noraristeromycin	126704	−102.03	−18.99	−8.82	−89.49
3	5′-Noraristeromycin analog	492117	−106.48	−18.44	−32.46	−92.27

Table 3 Docking energies of noraristeromycin inhibitors with pfSAHH

S. No.	Noraristeromycin inhibitors (Top scoring only)	CID	Binding with pfSAHH (kcal/mol)			
			Total Energy	H-Bond	v.d.w.	Steric
1	2-Fluoronoraristeromycin	9993207	−125.58	−16.28	−134.61	−269.23
2	5′-Noraristeromycin	126704	−108.50	−10.64	−113.93	−251.24
3	5′-Noraristeromycin analog	492117	−122.55	−11.81	−131.97	−269.28

not validated experimentally till now. Anti-malarial effect of curcumin may be due it's binding with pfSAHH.

To validate this hypothesis curcumin and its derivatives were docked with hsSAHH and pfSAHH. Docking energies of curcumin and its derivatives with hsSAHH and pfSAHH are given in Table 4 and Table 5. Curcumin and its derivatives have shown good binding affinity for hsSAHH, which is lower in comparison to pfSAHH. MolDock Score (docking energy) of curcumin for hsSAHH and pfSAHH is −119.49 kcal/mol and −161.69 kcal/mol respectively. Curcumin and its derivatives have very good affinity for target pfSAHH. The complex of curcumin and its derivative with pfSAHH is stabilized by significant contribution of hydrogen bonding. The pfSAHH can be a potent drug target against malaria because inhibition of pfSAHH enzyme prevents the DNA methylation leading to inhibition of protein expression from *Plasmodium falciparum*.

Docking results of curcumin and its derivatives with pfSAHH suggest that curcumin has very high affinity for binding with pfSAHH, and it forms a very low energy complex (−161.69 kcal/mol). Five hydrogen bonds with total H-bonding energy (−6.09 kcal/mol), are stabilizing the binding of curcumin with pfSAHH. Comparative analysis of binding of noraristeromycin and curcumin inhibitors with pfSAHH suggests that curcumin has very high affinity to bind with pfSAHH than its known inhibitors. This study clearly indicates that curcumin has very high binding affinity for pfSAHH and anti-malarial effect of curcumin may be due to its binding with pfSAHH. Curcumin and its derivative are predicted potent inhibitors of pfSAHH of *Plasmodium falciparum*. Curcumin, a strong and potent inhibitor of pfSAHH can inhibit the growth and development of *Plasmodium falciparum*.

3.4 Investigating the binding region of curcumin and 2-fluoronoraristeromycin with pfSAHH

MVD and its visualizer were used for interaction site analysis (Singh *et al.*, 2012). The interaction analysis for binding of 2-fluoronoraristeromycin and curcumin with pfSAHH has been done to find out the residues that are involved in binding. The 2-fluoronoraristeromycin shows very high affinity to bind with pfSAHH and it interacts with Leu53, His54, Thr56, Glu58, Glu200, Lys230, Asp234, Thr396, Gly397, His398, and Phe407 residues of pfSAHH. All these residues involved in binding with 2-fluoronoraristeromycin belong to the cavity-1. The 2-fluoronoraristeromycin forms 12 hydrogen bonds with the Glu58, Glu200, Lys230, Asp234, Gly397 and His398 residues of pfSAHH. The hydogen bonding is very significant for interaction of biomolecules. Curcumin forms very low binding energy complex with pfSAHH (−161.69 kcal/mol), that is much better in comparison to other curcumin derivatives and noraristeromycin inhibitors. Curcumin shows strong binding affinity with Leu53, His54, Thr56, Cys78, Asp134, Thr201, Lys230, Gly344, His345, Phe346, Leu389, Leu392, Gly397, His398 and Phe407 residues of pfSAHH. It also shows 5 hydrogen bonding with the Thr56, Thr201, Lys230 and Phe346 residues of pfSAHH. Interaction sites for binding of 2-fluoronoraristeromycin and curcumin with pfSAHH are given in Figs. 4(a) and 4(b).

The number of hydrogen bonds formed by curcumin is less than 2-fluoronoraristeromycin. There are total 11 amino acid residues of pfSAHH involed in interaction with the 2-fluoronoraristeromycin, whereas curcumin is showing interaction with 15 residues of pfSAHH. This indicates that curcumin shows not only higher affinity for pfSAHH but also increased number of interactions with amino acid residues of pfSAHH. Docking study

Table 4 Docking energies of curcumin and its derivative with hsSAHH

S. No.	Curcumin and its derivatives (Top scoring only)	CID	Binding with hsSAHH (kcal/mol)			
			Total Energy	H-Bond	v.d.w.	Steric score
1	Curcumin	969516	−119.44	−7.79	−48.48	−126.73
2	Monodemethoxy curcumin	5469424	−111.94	−7.93	−33.32	−120.24
3	Bis-demethoxy curcumin	5315472	−113.72	−13.10	30.34	−110.53
4	Allyl curcumin	16727530	−116.32	−5.19	−38.40	−122.48
5	Curcumin bis-acetate	6441419	−117.52	−2.50	−35.85	−126.23
6	Curcumin dimethyl ether	6477182	−117.33	−10.83	−35.51	−124.77

Table 5 Docking energies of curcumin and its derivative with pfSAHH

S. No.	Curcumin and its derivatives (Top scoring only)	CID	Binding with pfSAHH (kcal/mol)			
			Total Energy	H-Bond	v.d.w.	Steric score
1	Curcumin	969516	−161.69	−6.09	−164.86	−368.38
2	Monodemethoxy curcumin	5469424	−134.42	−7.67	−137.56	−338.35
3	Bis-demethoxy curcumin	5315472	−137.57	−6.07	−142.20	−308.32
4	Allyl curcumin	16727530	−149.99	−4.17	−155.18	−448.50
5	Curcumin bis-acetate	6441419	−159.71	−7.03	−163.74	−452.45
6	Curcumin dimethyl ether	6477182	−139.71	−4.79	−145.34	−396.43

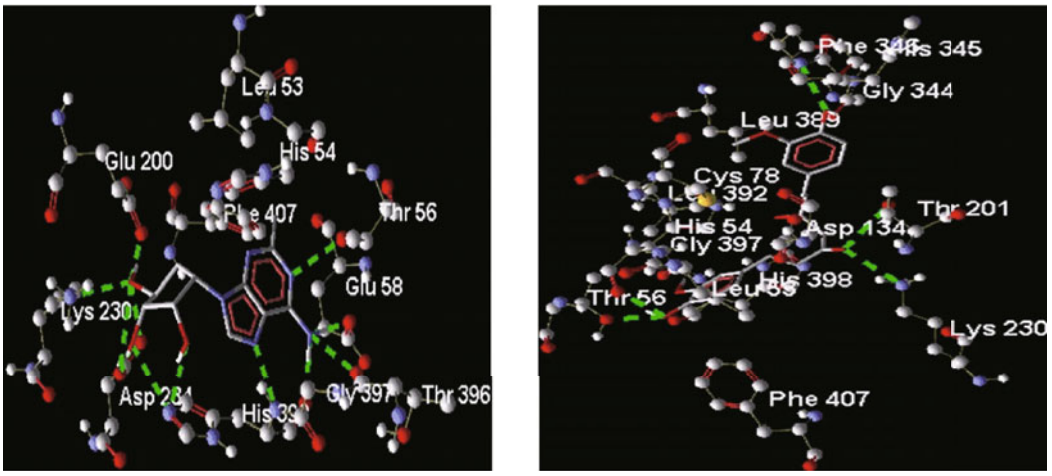

(a) (b)

Fig. 4 (a) 2-Fluoronoraristeromycin interaction with pfSAHH active site. (b) Curcumin interaction with pfSAHH active site. The amino acid residues are represented by ball and sticks, and the H-bonds are represented by dotted line.

indicates that seven amino acid residues *i.e.* Leu53, His54, Thr56, Lys230, Gly397, His398, Phe407 of pfSAHH are common in binding for both of the inhibitors. The residues of pfSAHH involved in binding with 2-fluoronoraristeromycin and curcumin are listed in Table 6.

It was reported that mutations of Cys59 residue in pfSAHH and Thr60 residue in hsSAHH causes remarkable impact on inhibition by 2-fluoronoraristeromycin. The steric hindrance between a functional group at the 2-position of an adenine nucleoside inhibitor and Thr60 of the hsSAHH enzyme is responsible for inhibitor selectivity for pfSAHH (Nakanishi *et al.*, 2005). It indicates that substitution of Cys59 by Thr in mutant pfSAHH results in similar sensitivity of mutant pfSAHH and hsSAHH for nucleoside inhibitors.

Cys59 amino acid residue may be associated with the binding region or it can affect the binding of 2-fluoronoraristeromycin with pfSAHH. 2-Fluoronoraristeromycin binds with Glu58 and Thr56, which are closer to Cys59 residue of pfSAHH. Curcumin interacts with the His54, Thr56 and Cys78 residues for binding, which are nearby residues of Cys59. Curcumin and noraristeromycin both bind within close proximity region of Cys59 of pfSAHH. Curcumin binds at the same binding site of pfSAHH with higher affin-

Table 6 Amino acid residues of pfSAHH involved in binding with 2-fluoronoraristeromycin and curcumin. Residues commom in binding for both inhibitors are shown in bold text

S. No.	Name of inhibitors	Residues (name and position) of pfSAHH involved in binding	No. of H-bonding
1	2-fluoronoraristeromycin	**Leu53, His54, Thr56**, Glu58, Glu200, **Lys230**, Asp234, Thr396, **Gly397, His398, Phe407**	12
2	Curcumin	**Leu53, His54, Thr56**, Cys78, Asp134, Thr201, **Lys230**, Gly344, His345, Phe346, Leu389, Leu392, **Gly397**, **His398, Phe407**	5

Table 7 Principal descriptors for inhibitors and their range in 95% of drugs

S. No	Principal descriptors	N1	N2	N3	C1	C2	C3	C4	C5	C6	Range 95% of drugs
1	MW	269.235	251.244	269.278	368.385	338.359	308.333	448.515	452.460	396.439	130/725
2	SASA	445.734	437.982	442.110	701.733	661.398	628.555	852.651	835.666	744.482	300/1000
3	FOSA	104.452	104.449	63.107	262.266	165.976	78.033	459.748	434.896	411.774	0/750
4	FISA	224.708	228.778	212.112	191.368	180.068	189.611	79.782	162.675	75.317	7/330
5	PISA	71.211	104.755	96.490	248.098	315.354	360.911	313.120	238.095	257.391	0/450
6	WPSA	45.363	0.000	70.402	0.000	0.000	0.000	0.000	0.000	0.000	0/175
7	MV	760.048	744.693	748.093	1204.341	1129.450	1055.061	1513.725	1473.029	1308.115	500/2000
8	PSA	123.820	123.859	117.877	113.116	105.252	97.988	84.029	143.175	76.891	7/200
9	rotatB	4.000	4.000	4.000	12.000	11.000	10.000	16.000	12.000	13.000	0/15
10	donorHB	5.000	5.000	4.800	2.000	2.000	2.000	0.000	0.000	0.000	0/6
11	accptHB	9.100	9.100	9.600	7.000	6.250	5.500	7.000	10.500	4.750	2/20
12	Glob	0.904	0.907	0.901	0.780	0.793	0.797	0.748	0.749	0.777	0.75/0.95

Notations: N1 = 2-fluoronoraristeromycin, N2= 5′-noraristeromycin, N3 = 5′-noraristeromycin analog, C1 = curcumin, C2 = monodemethoxy curcumin, C3 = bis-demethoxy curcumin, C4 = allyl curcumin, C5 = curcumin bis-acetate, C6 = curcumin dimethyl ether.

ity than 2-fluoronoraristeromycin. So curcumin can inhibit the activity of pfSAHH much better than 2-fluoronoraristeromycin. It can be concluded that antimalarial effect of curcumin may be due to its binding with pfSAHH. Curcumin may be used as a lead compound to prepare much potent inhibitors of pfSAHH.

3.5 Principal descriptors and ADME analysis

Twelve principal descriptors and twenty predicted ADME properties were calculted for inhibiotrs by QikProp software (Yadav *et. al.*, 2010; Yadav *et al.*, 2011). Principal descriptors for inhibitors and their range in 95% of drugs are given in Table 7. Following principal descriptors are included in the study: Molecular Weight (MW), Total solvent accessible surface area (SASA), Hydrophobic SASA (FOSA), Hydrophilic SASA (FISA), Carbon Pi SASA (PISA), Weakly Polar SASA (WPSA), Molecular Volume (MV), van der Waals Polar SA (PSA), No. of Rotatable Bonds (rotatB), Donor-Hydrogen Bonds (donorHB), Acceptor-Hydrogen Bonds (accptHB) and Globularity (Glob) (Singh *et al.*, 2013).

Total solvent accessible surface area (SASA in Å^2) was calculated using a probe with a 1.4 Å radius. Curcumin and its derivatives have higher SASA (628.55–852.651 Å^2), as compared to noraristeromycin inhibitors (437.982–445.734 Å^2). In 95% of drugs total SASA ranges from 300–1000 Å^2. Curcumin and its derivatives have more hydrophobic and less hydrophilic solvent accessible surface areas than noraristeromycin inhibitors. Similarly in 95% drugs, MV varies from 500–2000 Å^3, which is high in case of curcumin derivatives (1055.061–1513.725 Å^3) and closer to the range expected in majority of drugs. PSA is formed by van der Waals surface area of polar nitrogen and oxygen atoms. It predicts the passive transport of molecules through membranes and is related to the bioavailability of drug. For a molecule to have good oral bioavailability, PSA should be less than 140 Å^2 (Ertl *et al.*, 2000). As for globularity descriptor (4πr2)/(SASA), r is the radius of a sphere with a volume equal to the molecular volume. Glob value, in case of noraristeromycin inhibiotrs was found higher (0.901–0.907) than curcumin derivatives (0.748–0.797). Globularity is 1.0 for a spherical molecule. The normal range of Glob for most of the drugs is 0.75–0.95.

A large number of ADME properties (Meena *et al.*, 2011; Komal *et al.*, 2011) such as Polarizability in cubic angstroms (Polrz), logP for hexadecane/gas

Table 8 Predicted ADME properties for inhibitors and their range in 95% of drugs

S. No	Properties predictions	N1	N2	N3	C1	C2	C3	C4	C5	C6	Range 95% of drugs
1	Polrz	22.375M	22.081M	22.138M	36.708M	34.995M	33.095M	47.142M	47.365M	40.308M	13/70
2	LogPC16	8.378M	8.812M	9.077M	13.027M	12.656M	12.298M	15.429M	15.082M	12.843M	4/18
3	LogPoct	20.145M	19.939M	19.991M	19.091M	18.189M	17.412M	18.461M	21.594M	15.201M	8/35
4	LogPw	18.225M	18.446M	18.510M	11.574M	11.340M	11.117M	7.809M	12.152M	5.585M	4/45
5	LogPo/w	−0.951	−1.178	−0.915	2.735	2.736	2.559	5.576	2.945	5.296	−2.0/6.5
6	LogS	−2.001	−1.737	−2.052	−4.503	−4.220	−4.054	−6.105	−4.602	−5.722	−6.5/0.5
7	CIlogS	−1.909	−1.660	−1.846	−4.616	−4.308	−3.996	−6.070	−4.531	−6.008	−6.5/0.5
8	LogKhsa	−0.723	−0.733	−0.771	−0.026	−0.032	−0.048	0.460	−0.424	0.593	−1.5/1.5
9	Log BB	−1.401	−1.531	−1.245	−2.256	−2.008	−2.027	−1.352	−2.092	−1.052	−3.0/1.2
10	Metab	3	4	5	5	4	3	7	3	4	1.0/8.0
11	CNS	−2	−2	−2	−2	−2	−2	−2	−2	−2	−2 inactive, +2 active
12	LogHERG	−3.431	−3.533	−3.587	−6.273	−6.385	−6.532	−7.107	−6.725	−6.368	concern below −5
13	PCaco	73	67	96	151	194	157	1735	283	1912	< 25 poor, >500 great
14	PMDCK	52	26	96	64	84	67	897	126	997	< 25 poor, >500 great
15	Log Kp	−5.026	−4.983	−4.705	−3.020	−2.671	−2.783	−0.351	−2.527	−0.753	$-8.0/-1.0$ Kp cm hr^{-1}
16	Jm	0.025	0.048	0.047	0.011	0.043	0.045	0.157	0.034	0.133	μg $cm^{-2}hr^{-1}$
17	Rule of 5	0	0	0	0	0	0	1	0	1	max. 4
18	Rule of 3	0	0	0	0	0	0	2	0	1	max. 3
19	PHOA	55	53	57	82	84	81	100	88	100	< 25% is poor
20	QmHOA	Medium	Medium	Medium	Medium	High	High	Low	High	High	> 80% is High

(logPC16), logP for octanol/gas (logPoct), log P for water/gas (logPw), log P for octanol/water (logPo/w), logS for aqueous solubility (logS), logS-conformation independent (CIlogS), log Khsa serum protein binding (logKhsa), log BB for brain/blood (logBB), No. of primary metabolites (Metab), Predicted central nervous system activity (CNS), HERG K^+ channel blockage: log IC_{50} (logHERG), apparent Caco-2 permeability in nm/sec (PCaco), apparent MDCK permeability in nm/sec (PMDCK), QP log Kp for skin permeability (logKp), maximum transdermal transport rate (Jm), Lipinski rule of 5 violations (rule of 5), Jorgensen rule of 3 violations (rule of 3), percentage human oral absorption in GI (pHOA), qualitative model for human oral absorption (QmHOA) were calculated. Predicted ADME properties for inhibitors and their range in 95% of drugs are given in Table 8.

The normal range of polarizability is from 13–70 M, which is better and higher in curcumin derivatives (33.095–47.142 M) than noraristeromycin inhibitors (22.0). The range of logP for octanol /water in 95% drugs is −2.0–6.5, which is negative in noraristeromycin inhibitors (−0.915 to −1.178) and positively high in curcumin derivatives (2.559–5.576). The log BB for brain/blood (range in 95% drugs −3.0–1.2) is higher for noraristeromycin inhibitors than curcumin derivatives. The IC_{50} represents the concentration of a drug that is required for 50% inhibition *in vitro* (Pajeva *et al.*, 2009). The logHERG (log IC_{50}) values for curcumin derivatives are (−6.273 to −7.107), which are less than noraristeromycin (−3.431 to −3.587). The negative value of logHERG indicates that the lower is the value of logHERG, the lesser is the blockage of K+ ion channels.

CNS is predicted on −2 (inactive) to +2 (active) scales, which is found inactive in all inhibitors. The logHERG value for 95% drugs is concern if it is less than −5. The prediction of human oral absorption is based on quantitative multiple linear regression model. PCaco and PMDCK descriptors are used for prediction of non-active transport, and found high in curcumin derivatives as compared to noraristeromycin. PCaco (1912 nm/sec) and PMDCK (997 nm/sec) values are very high in curcumin dimethyl ether, which is consid-

Table 9 Predicted toxicity of noraristeromycin and curcumin derivatives

S. No	Inhibitors	MRTD (mg/kg/day)	hERG_Filter	hERG (mol/L)	CABR	PHOS	AlkPhos	GGT	LDH	SGOT
1	2-Fluoronoraristeromycin	< 3.16	NT	3.66	T	NT	NT	NT	T	T
2	5′-Noraristeromycin	< 3.16	NT	3.72	T	NT	NT	NT	T	T
3	5′-Noraristeromycin analog	< 3.16	NT	3.57	T	NT	NT	NT	T	T
4	Curcumin	< 3.16	NT	4.98	NT	NT	NT	T	NT	T
5	Monodemethoxy curcumin	> 3.16	NT	4.9	T	NT	T	T	NT	T
6	Bis-demethoxy curcumin	< 3.16	NT	5.28	T	NT	T	T	NT	NT
7	Allyl curcumin	> 3.16	NT	5.37	NT	NT	T	T	NT	T
8	Curcumin bis-acetate	> 3.16	NT	5.51	NT	NT	T	T	NT	T
9	Curcumin dimethyl ether	> 3.16	NT	5	NT	NT	T	T	NT	T

NT = Nontoxic, T=Toxic.

ered excellent in case greater than 500. All inhibitors are satisfying the Lipinski rule's of five and Jorgensen's rule of three (logs > -5.7, PCaco > 22 nm/s, Primary metabolite < 7), except allyl curcumin and curcumin dimethyl ether. Compounds that satisfy the Lipinski rule's of five are considered drug-like (Lipinski *et al.*, 2001). Compounds with no violations of Jorgensen's rule of three are more likely to be orally available. Percentage human oral (pHOA) of inhibitors in gastro intestine may vary (±20%). Curcumin and its derivatives have better oral absorption in gastro intestine than noraristeromycin. 2-Fluoronoraristeromycin, 5′-noraristeromycin and 5′-noraristeromycin analogues are not good qualitative models for human oral absorption as the pHOA value is less than 80%. In case of curcumin and its derivatives the pHOA value is more than 80%. So curcumin and its derivatives can serve as a good qualitative model for human oral absorption. But ADME properties are not in favor of allyl curcumin, which may not be a potent drug candidate. ADME properties are very important for a molecule to serve as a drug (Wang, 2009). Value of principal descriptors and ADME prediction for curcumin and its derivatives are closer to the drug-like compounds.

3.6 Toxicity analysis

Predicted toxicity values for curcumin and noraristeromycin inhibitors are given in Table 9. MRTD is a qualitative assessment of the Maximum Recommended Therapeutic Dose administered as an oral dose. MRTD value, lower than 3.16 indicates an "active" compound with significant potential for side effects. MRTD higher than 3.16 specifies an "inactive" compound with fewer side effects (Matthews *et al.*, 2004a). MRTD value is lower than 3.16 mg/kg/day for curcumin as well as for noraristeromycin inhibitors and higher than 3.16 mg/kg/day for other curcumin derivatives.

The hERG gene encodes potassium channels, which are responsible for the normal repolarization of the cardiac action potential. Blockage or any other impairment of these channels in the heart cells can lead to fatal cardiac arrhythmias (Sanguinetti *et al.*, 2006). Affinity towards hERG K^+ channel and potential for cardiac toxicity is measured in terms of hERG (mol/L). Compounds with an $IC_{50} \leq 10$ μmol/L were labeled as "Toxic", while those > 10 μmol/L were considered as "Nontoxic". "Toxic" indicates that a compound is capable of blocking the hERG channel. The hERG (pIC_{50}) concentration is higher for curcumin derivatives than noraristeromycin inhibitors. Curcumin and noraristeromycin inhibitor were found less toxic effect on heart (http://www.simulations-plus.com).

CABR measures the qualitative estimation of triggering the mutagenic chromosomal aberrations (CA) in response to a drug or molecule. Noraristeromycin inhibitors, mono and bis-demethoxy curcumin have predicted mutagenic capability, while curcumin and other curcumin derivatives are predicted non-mutagenic agents. PHOS predicts the qualitative estimation of causing phospholipidosis. Phospholipidosis is a lysosomal storage disorder characterized by the accumulation of phospholipids in the tissues of the body. The presence of phospholipids may disrupt neuronal cell signaling (Lowe *et al.*, 2010). Noraristeromycin and curcumin derivatives were predicted as incapable of inducing phospholipidosis.

Adverse effect to human liver is predicted due to elevation at the level of alkaline phosphatase (AlkPhos), gamma-glutamyltransferase (GGT), lactate dehydrogenase (LDH) and serum glutamate oxaloacetate transaminase (SGOT) (Matthews *et al.*, 2004b). Elevation at the level of alkaline phosphatase (AlkPhos) along with (SGOT) or serum glutamate pyruvate transaminase (SGPT) may cause hepatic injury (Mithani *et al.*, 1996). Noraristeromycin inhibitors have nontoxic effect on PHOS, AlkPhos and GGT, but toxic to LDH and SGOT. Curcumin and its derivatives have shown nontoxic effect on LDH. Based on toxicity prediction, we concluded that curcumin had no cardiac

toxicity (hERG blockage), mutagenesis, phospholipidosis, and liver toxicity due to elevation at the level of alkaline phosphatase and LDH, but may have liver toxicity due to elevation at the level of GGT and SGOT.

4 Conclusion

The present *in silico* studies provide insight into the inhibition of pfSAHH by curcumin and its derivatives. Docking study suggests that curcumin has high binding affinity for pfSAHH, which is much higher than the known inhibitors. Curcumin and noraristeromycin inhibitors have shown good hydrophobic interaction with active site of pfSAHH, which is also related to the binding of NAD and ADN, which implies that binding of curcumin with pfSAHH might inhibit the normal function of pfSAHH enzyme, and finally result in anti-malarial effect. This study indicates that pfSAHH may be used as a molecular drug target for curcumin against malaria. Curcumin can be used as a natural lead compound for designing more effective inhibitors of pfSAHH. These pfSAHH inhibitors are expected to provide a potent chemotherapeutic agent against malaria. Curcumin was predicted to be the most potent inhibitor amongst all the derivatives taken for study with favorable druggability and ADMET properties, compared to noraristeromycin inhibitors. Though SAHH enzyme is common in *Plasmodium falciparum* and human, yet slight structural differences such as single amino acid variation causes selective inhibition of pfSAHH. Therefore, pfSAHH might be suitable target for designing anti-malarial drugs.

References

[1] Ando, T., Kojima, K., Chahota, P., Kozaki, A., Milind, N.D., Kitade, Y. 2008. Synthesis of 4′-modified noraristeromycins to clarify the effect of the 4′-hydroxyl groups for inhibitory activity against S-adenosyl-l-homocysteine hydrolase. Bioorg Med Chem Lett 18, 2615–2618.

[2] Brady, R.L., Cameron, A. 2004. Structure-based approaches to the development of novel anti-malarials. Curr Drug Targets, 137–149.

[3] Efferth, T., Herrmann, F., Tahrani, A., Wink, M. 2011. Cytotoxic activity of secondary metabolites derived from Artemisia annua L. towards cancer cells in comparison to its designated active constituent artemisinin. Phytomedicine 18, 959–969.

[4] Ertl, P., Rohde, B., Selzer, P. 2000. Fast calculation of molecular polar surface area as a sum of fragment based contributions and its application to the prediction of drug transport properties. J Med Chem 43, 3714–3417.

[5] Garah, F.B., Stigliani, J.L., Cosldan, F., Meunier, B., Robert, A. 2009. Docking studies of structurally diverse antimalarial drugs targeting PfATP6: No correlation between in silico binding affinity and *in vitro* antimalarial activity. ChemMedChem 4, 1469–1479.

[6] Ji, H.F., Shen, L. 2009. Interactions of curcumin with the PfATP6 model and the implications for its antimalarial mechanism. Bioorg Med Chem Lett 19, 2453–2455.

[7] Jorgensen, W.L. 1998. BOSS - Biochemical and organic simulation system. In: Schleyer, P.V.R. (Ed.) The Encyclopedia of Computational Chemistry, John Wiley & Sons Ltd., Athens, USA, 3281–3285.

[8] Jung, M., Kim, H., Nam, K.Y., No, K.T. 2005. Three-dimensional structure of Plasmodium falciparum Ca^{2+}-ATPase (PfATP6) and docking of artemisinin derivatives to PfATP6. Bioorg Med Chem Lett 15, 2994–2997.

[9] Kalani, K., Yadav, D.K., Khan, F., Srivastava, S.K., Suri, N. 2011. Pharmacophore, QSAR and ADME based semi-synthesis and *in-vitro* evaluation of ursolic acid analogs for anti-cancer activity. J Mol Model 8, 3389–3413.

[10] Kitade, Y., Kozaki, A., Miwa, T., Nakanishi, M., Yatome, C. 2000. Synthesis of carbocyclic nucleosides and their SAH hydrolase inhibitory activities. Nucleic Acids Symp Ser 44, 111–112.

[11] Kitade, Y., Kojima, H., Zulfiqur, F., Kim, H.S., Wataya, Y. 2003a. Synthesis of 2-fluoronoraristeromycin and its inhibitory activity against Plasmodium falciparum S-adenosyl-L-homocysteine hydrolase. Bioorg Med Chem Lett 13, 3963–3965.

[12] Kitade, Y., Kojima, H., Zulfiqur, F., Yabe, S., Yamagiwa, D., Ito, Y., Nakanishi, M., Ueno, Y., Kim, H.S., Wataya, Y. 2003b. Synthesis of carbocyclic and acyclic nucleosides possessing 2-fluoroadenine derivatives and their inhibitory activities against Plasmodium falciparum SAH hydrolase. Nucl Acid Res (Suppl. 3), 5–6.

[13] Kojima, H., Yamaguchi, T., Kozaki, A., Nakanishi, M., Ueno, Y., Kitade, Y. 2002. Synthesis of noraristeromycin analogues possessing SAH hydrolase inhibitory activity for the development of antimalaria agents. Nucl Acid Res (Suppl. 2), 141–142.

[14] Lipinski, C.A., Lombardo, F., Dominy, B.W., Feney, P.J. 2001. Experimental and computational approaches to estimate solubility and permeability in drug discovery and development settings. Adv Drug Deliv Rev 46, 3–26.

[15] Lowe, R., Glen, R., Mitchell, J.B.O. 2010. Predicting phospholipidosis using machine learning. Mol Pharm 7, 1708–1714.

[16] Matthews, E.J., Kruhlak, N.L., Benz, R.D., Contrera, J.F. 2004a. Assessment of the health effects of chemicals in humans: I. QSAR estimation of the maximum recommended therapeutic dose (MRTD) and no effect level (NOEL) of organic chemicals based on clinical trial data. Curr Drug Disc Tech 1, 61–76.

[17] Matthews, E.J., Kruhlak, N.L., Weaver, J.L., Benz, R.D., Contrera, J.F. 2004b. Assessment of the health effects of chemicals in humans: II. Construction of an adverse effects database for QSAR modeling. Curr Drug Disc Tech 1, 243–254.

[18] Meena, A., Yadav, D.K., Srivastava, A., Khan, F., Chanda, D, Chattopadhyay, S.K. 2011. *In silico* exploration of anti-inflammatory activity of natural Coumarinolignoids. Chem Biol Drug Des 78, 567–579.

[19] Mimche, P.N., Taramelli, D., Vivas, L. 2011. The plant-based immunomodulator curcumin as a potential candidate for the development of an adjunctive therapy for cerebral malaria. Malar J 15, 10 Suppl 1, S10.

[20] Mithani, S.D., Bakatselou, V., TenHoor, C.N., Dressman, J.B. 1996. Estimation of the increase in solubility of drugs as a function of bile salt concentration. Pharm Res 13, 163–167.

[21] Naik, P.K., Srivastava, M., Bajaj, P., Jain, S., Dubey, A., Ranjan, P., Kumar, R., Singh, H. 2011. The binding modes and binding affinities of artemisinin derivatives with Plasmodium falciparum Ca^{2+}-ATPase (PfATP6). J Mol Model 17, 333–357.

[22] Nakanishi, M., Yabe, S., Tanaka, N., Ito, Y., Nakamura, K.T., Kitade, Y. 2005. Mutational analyses of Plasmodium falciparum and human S-adenosylhomocysteine hydrolases. Mol Biochem Parasitol 143, 146–151.

[23] Padmanaban, G., Nagaraj, V.A., Rangarajan, P.N. 2007. Drugs and drug targets against malaria. Curr Sci 92, 1545–1555.

[24] Pajeva, I.K., Globisch, C., Wiese, M. 2009. Combined pharmacophore modeling, docking, and 3D QSAR studies of ABCB1 and ABCC1 transporter inhibitors. Chem Med Chem 4, 1883–1896.

[25] Rasoanaivo, P., Wright, C.W., Willcox, M.L., Gilbert, B. 2011. Whole plant extracts versus single compounds for the treatment of malaria: Synergy and positive interactions. Malar J 15, 10 Suppl 1, S4.

[26] Reddy, R.C., Vatsala, P.G., Keshamouni, V.G., Padmanaban, G., Rangarajan, P.N. 2005. Curcumin for malaria therapy. Biochem Biophys Res Commun 326, 472–474.

[27] Sadowski, J., Gasteiger, J., Klebe, G. 1994. Comparison of automatic three-dimensional model builders using 639 X-ray structures. J Chem Inf Comput Sci 34, 1000–1008.

[28] Sanguinetti, M.C., Tristani-Firouzi, M. 2006. hERG potassium channels and cardiac arrhythmia. Nature 440, 463–469.

[29] Sharma, S.K., Kapoor, M., Ramya, T.N., Kumar, S., Kumar, G., Modak, R., Sharma, S., Surolia, N., Surolia, A. 2003. Identification, characterization, and inhibition of Plasmodium falciparum beta-hydroxyacyl-acyl carrier protein dehydratase (FabZ). J Biol Chem 278, 45661–45671.

[30] Shi, W., Ting, L.M., Kicska, G.A., Lewandowicz, A., Tyler, P.C., Evans, G.B., Furneaux, R.H., Kim, K., Almo, S.C., Schramm, V.L. 2004. Plasmodium falciparum purine nucleoside phosphorylase:crystal structures, immucillin inhibitors, and dual catalytic function. J Biol Chem 279, 18103–18106.

[31] Singh, D.V., Agarwal, S., Kesharwani, R.K., Misra, K. 2012. Molecular modeling and computational simulation of the photosystem-II reaction center to address isoproturon resistance in Phalaris minor. J Mol Model 18, 3903–3913.

[32] Singh, D.B., Gupta, M.K., Kesharwani, R.K., Misra, K. 2013. Comparative docking and ADMET study of some curcumin derivatives and herbal congeners targeting β-amyloid. Netw Model Anal Health Inform Bioinforma 2, 13-27.

[33] Tagboto, S., Townson, S. 2001. Antiparasitic properties of medicinal plants and other naturally occurring products. Adv Parasitol 50, 199–295.

[34] Tanaka, N., Nakanishi, M., Kusakabe, Y., Shiraiwa, K., Yabe, S., Ito, Y., Kitade, Y., Nakamura, K.T. 2004. Crystal structure of S-adenosyl-L-homocysteine hydrolase from the human malaria parasite Plasmodium falciparum. J Mol Biol 343, 1007–1017.

[35] Thomsen, R., Christensen, M.H. 2006. MolDock: A new technique for high-accuracy molecular docking. J Med Chem 49, 3315–3321.

[36] Tschan, S., Mordmller, B., Kun, J.F. 2011. Threonine peptidases as drug targets against malaria. Expert Opin Ther Targets, 365–378.

[37] Wang, J. 2009. Comprehensive assessment of ADME risks in drug discovery. Curr Pharm 15, 2195–2219.

[38] Yadav, D.K., Khan, F., Negi, A.S. 2011. Pharmacophore modeling, molecular docking, QSAR, and *in silico* ADMET studies of gallic acid derivatives for immunomodulatory activity. J Mol Model 18, 2513–2525.

[39] Yadav, D.K., Meena, A., Srivastava, A., Chanda, D., Khan, F., Chattopadhyay, S.K. 2010. Development of QSAR model for immunomodulatory activity of natural Coumarinolignoids. Drug Design, Development & Therapy 4, 173–186.

[40] Yang, J., Chen, C. 2004. GEMDOCK: A generic evolutionary method for molecular docking. Proteins 55, 288–304.

[41] Yang, X., Hu, Y., Yin, D.H., Turner, M.A., Wang, M., Borchardt, R.T., Howell, P.L., Kuczera, K., Schowen, R.L. 2003. Catalytic strategy of S-adenosyl-L-homocysteine hydrolase: Transition-state stabilization and the avoidance of abortive reactions. Biochemistry 42, 1900–1909.

[42] Yuan, C.S., Saso, Y., Lazarides, E., Borchardt, R.T., Robins, M.J. 1999. Recent advances in S-adenosyl-L-homocysteine hydrolase inhibitors and their potential clinical applications. Expert Opin Ther Patents 9, 1197–1206.